OPEN ACCESS

Kashf Journal of Multidisciplinary Research
Vol: 02 - Issue 2 (2025)
P-ISSN: 3007-1992 E-ISSN: 3007-200X
https://kjmr.com.pk

Chemical Coprecipitation Synthesis and Enhanced Photocatalytic Characteristics of Nickel-doped Zinc Sulfide Nanoparticles

Muhammad Iqbal
Faculty of Sciences, The Superior University, Lahore iqbalphy335@gmail.com
Zeeshan Mahmood
Faculty of Sciences, The Superior University, Lahore
Waseem Sajjad Tahir
Faculty of Sciences, The Superior University, Lahore
Kanwal Akhtar
Faculty of Sciences, The Superior University, Lahore
Muhammad Salman
Faculty of Sciences, The Superior University, Lahore
Aurangzaib
Faculty of Sciences, The Superior University, Lahore
Aneela Din Muhammad
Faculty of Sciences, The Superior University, Lahore
Yasir Javeed
Department of Physics, University of Agriculture, Faisalabad, Pakistan

**Corresponding author:*
DOI: https://doi.org/10.71146/kjmr263

Article Info

Abstract

Metal sulfide semiconductors having wide bandgap like ZnS experience a significant decrease in band gap when transition metal ions like $Ni2^{+}$ are doped. This alteration creates new composite materials with various uses in photonics, solar cells, optoelectronic devices, and spintronic devices. These modifications have led to improvements in ZnS nanoparticle production techniques. Nickel-doped zinc sulfide nanoparticles are synthesized by using a simple chemical coprecipitation method. Ni-doped ZnS nanoparticles have been characterized using UV-visible spectra and Fourier-transform infrared spectroscopy. Zn–S vibrational bands were detected by Fourier-transform infrared (FTIR) spectroscopy; changes in these bands suggested that Ni had been successfully incorporated into the ZnS lattice. UV–visible spectroscopy revealed a decrease in the optical band gap from 3.70 eV for 3% Ni-doped ZnS to 3.46 eV for 1% Ni-doped ZnS, demonstrating tunable optical properties due to Ni doping, which could enhance photocatalytic performance under visible light.

Keywords: *Combining ability, Heterosis study, Gene action, Heritability, Inbreeding depression.*

Introduction

Nanoscale semiconductor materials have gained significant attention in recent years due to their distinctive physical and chemical properties [1]. Nanoscale semiconductors undergo substantial changes in their characteristics due to the size quantization effect, which is more noticeable than their bulk counterparts. Regarding quantum dots, once their diameter is lowered below a critical limit (the Bohr radius), size confinement also plays a significant role in identifying energy levels [2]. The II-VI material categories contain a wide range of unique compounds, including bulk materials, thin films, microcrystalline forms, and nanostructures [3], [4], [5]. These materials can have varied surface configurations and include different kinds of anions (negatively charged ions) and cations (positively charged ions). Changes in these characteristics can significantly impact the material's electrical and optical characteristics [6], [7], [8]. The chemical composition, size, and microstructure may need to be precisely adjusted to enable the adjustment of these properties in systems designed for specific optoelectronic or photonic applications. The required property alteration can be created in a variety of ways, depending on its particulars. Local electrical state fluctuation may be the only significant factor in some devices, such as switching or laser devices. The distinct electrical, optical, and catalytic characteristics of metal sulfides, including ZnS, MoS2, CdS, and WS2, have made them essential materials for energy-related applications [9]. The employment of these materials in energy-conversion and storage technologies, such as battery electrodes, electrocatalysis, and photocatalysis, is very appealing. Metal sulfides, such as CdS and ZnS, are well-known in photocatalysis for their capacity to absorb visible light and promote charge separation, making them ideal for hydrogen evolution reactions (HERs) and general water splitting. That being said, MoS2 and WS2 are well known for having superior catalytic activity in HERs because of their layered architectures, which facilitate effective electron transport and offer many active sites for hydrogen adsorption [10]. Furthermore, these sulfides' high surface area and adjustable band gaps improve their efficiency in converting solar energy into chemical energy. Metal sulfides are considered excellent possibilities for next-generation lithium-ion and sodium-ion batteries because of their large theoretical capacity and superior conductivity. Metal sulfides' diverse range of uses makes them essential building blocks for the creation of sustainable energy systems [11].

The sphalerite, the cubic (zinc blende) structure of ZnS, is stable at room temperature while, wurtzite a less dense hexagonal structure, is stable at 1020°C at atmospheric pressure. With a broad bandgap of 3.7 eV and a significant exciton binding energy of 40 meV, ZnS is a prominent II-VI semiconductor that is essential for semiconductor applications [12], [13]. ZnS offers a wide range of potential applications because of its unique characteristics [14] as optoelectronic devices, e.g., photoconductors, optical sensors, light–emitting materials, solid-state solar window layers, and field-effect transistors [15], [16], [17], [18], [19].One promising property of ZnS nanoparticles is their capacity to modify the band gap energy by varying the particle size. An extended band gap is seen in particles with diameters between 2 and 4 nm, indicating that the ZnS nanoparticles' band gap has increased. Because of this feature, they can be used to apply UV protection coatings on polymers and other materials. To efficiently absorb strong UV radiation, zinc sulfide (ZnS) can be used to create ultraviolet (UV) sensors. It is a good alternative to organic UV sensors because of its non-toxicity and water stability. When compared to other sulfides and oxides, zinc sulfide (ZnS) is known for having better electroluminescent qualities. This is because it emits a bright, colorless light when electrically activated. Because III-V semiconductors and organic materials can emit

certain light wavelengths, they are ideal for the advancement of white LED technology. Furthermore, ZnS nanoparticles have unique electrical and optical characteristics that may be greatly adjusted by doping, particle size management, and surface modification in contrast to other sulfides like MoS2, CdS, and WS2. In photocatalytic systems, especially hydrogen evolution reactions (HERs), where effective charge separation and transfer are critical, this tunability is vital for increasing their efficiency [20]. In recent years, metal sulfides—including ZnS—have drawn a lot of attention because of their capacity to lower overpotentials and enhance the kinetics of HERs, which is critical in the creation of clean hydrogen fuel [20], [21]. The versatile nature of ZnS nanoparticles in contrast to other sulfides is also highlighted in the introduction. Despite their high catalytic activity, sulfides such as MoS2 and CdS frequently have stability problems and rapid recombination of photogenerated charge carriers. ZnS offers a strong substitute that can be tuned for better photocatalytic performance because of its increased stability and doping-adjustable characteristics. Several researchers are very interested in the technique of adding transition metals to micro- and nano-ZnS [22]. Superior characteristics of doped ZnS nanoparticles over undoped and bulk ZnS vary based on the dopant employed. Numerous aspects of ZnS, including its crystal structure, grain formation behavior, particle size distribution, stability, optical and electrical conductivity, and magnetic properties, can be altered by the addition of a dopant. Gas sensors, light-emitting diodes, solar cells, transparent conductive films, field-emission displays, varistors, photocatalysts, and lithium batteries were among the various applications for doped ZnS.

In this research, we strive to investigate the optical, morphological, and structural characteristics of ZnS particles doped with Ni2+. Various approaches such as gamma irradiation [23], chemical precipitation (Yang et al., 2002), mechano-chemical [26], hydrothermal [24], sol-gel [27], and reverse Michelle's methods [28], can be used to synthesize divalent elements like Ni2+ ions doped ZnS nanocrystals. We favored the co-precipitation approach for synthesizing ZnS because of its simplicity of use, affordability, and equipment accessibility (Godavarti et al., 2016). TEM is used to examine the shape and size of the particles. FTIR spectroscopy is used to investigate the functional groups of ZnS and Ni.

Experimental

Pure and Ni-doped ZnS nanoparticles were prepared by using the chemical coprecipitation method. All chemicals used were of analytical grade purity. Chemicals required to prepare pure and Ni-doped ZnS nanomaterials were Zinc chloride (ZnCl2), thiourea (SC(NH2)2), and nickel chloride (NiCl2). Zinc chloride (0.5 M) was added to 200 mL of distilled water and thiourea (1 M) to 200 mL of distilled water in a separate beaker. After 25 minutes of stirring in both beakers, ZnCl2 solution was added drop by drop to the thiourea solution with constant magnetic stirring. To make the precipitate few grains of NaOH were added which increased the PH value of solution from 5 to 8. The solution was placed in an overnight magnetic stirrer. The next day, the solution was washed several times with distilled water by a centrifuge machine to remove impurities. In this way, precipitates of pure ZnS were obtained. ZnS was added to the crucible and placed at 80 oC for overnight drying, to remove both water and organic capping agent and other by-products formed during the reaction process. After grinding, the sample was added to a falcon tube. Then ZnS doped with Ni was prepared, by varying Ni concentrations of 1%, and 3% using the same method.

Results and discussion

3.1 Absorption spectra of prepared samples

UV-visible absorption spectra of nickel-doped ZnS nanoparticles are shown in Figure 1, recorded in the 200–800 nm wavelength region. 1% Ni-doped ZnS showed absorption at a wavelength of 276 nm, and 3% Ni-doped ZnS showed two peaks at 231 nm and 678 nm wavelengths.

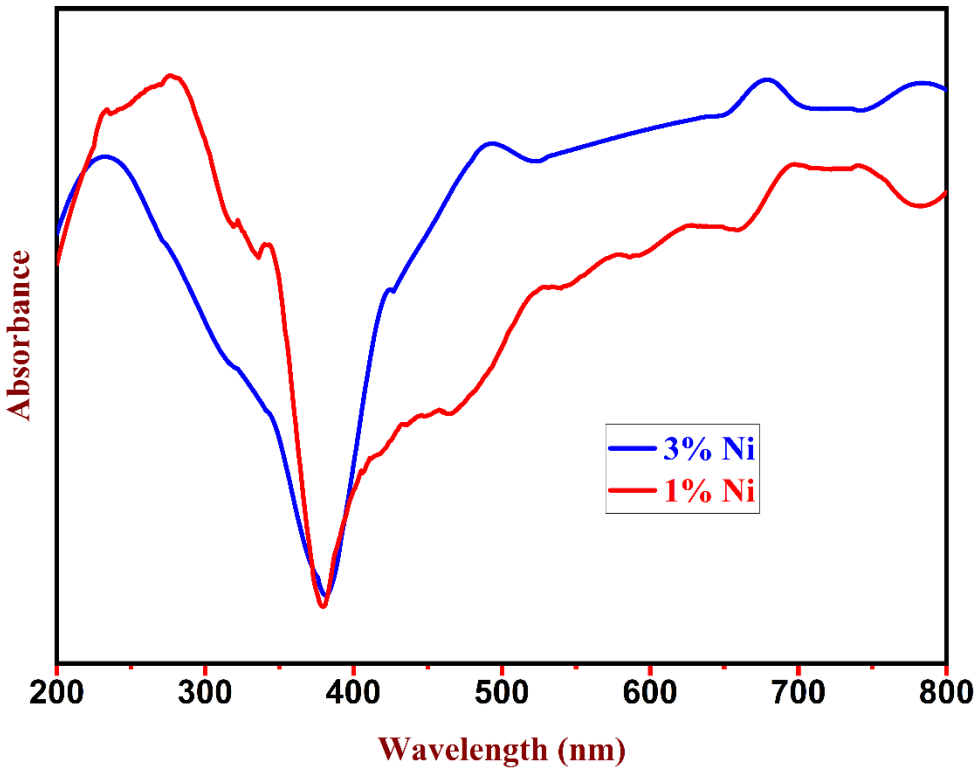

Figure 1. Optical absorption spectra of 1% and 3% Ni-doped ZnS.

Compared to the absorption wavelength for 1% Ni-doped ZnS nanoparticles, the sample showed a significant absorption wavelength for 3% Ni-doped ZnS nanoparticles, indicating a blue shift caused by the nanoparticles' quantum confinement effect. Many factors, including oxygen deficit, d-d transitions, impurity centers, particle size, lattice distortion ratio, and surface roughness, can also affect absorbance [29].

3.2 Energy bandgap spectra of prepared samples

An essential characteristic of semiconductors is the optical band gap, which is the energy difference between the empty conduction band maximum (CBM) and the filled valence band minimum (VBM). The optical absorption edge is a sharp feature in the optical spectrum that results from the strong optical excitation of electrons across the optical band gap. The samples' bandgap energy is determined by plotting (Ah$\boldsymbol{\nu}$)1/ $\boldsymbol{\gamma}$ versus Energy = h$\boldsymbol{\nu}$. The energy bandgap value is obtained by linearly fitting the straight part of the curve on the hü axis, also known as the energy

axis. Wood and Tauc's equation provides the relationship between the incident photon energy (h**ν**) and the absorption coefficient (α).

$$(\alpha h\nu)1/\gamma = A\,(h\nu - Eg)$$

Key factors in this formula are h (Planck's constant), v (photon frequency), Eg (optical band gap energy), and A (constant) which are used to estimate the absorption coefficient (α) for nanoparticles. The γ factor, which determines the electron transition type, takes on a value of 1/2 or 2 for direct and indirect transition band gaps. By plotting the value of $(\alpha h\nu)$ $1/\gamma$ with $h\nu$ and then extrapolating in the linear area over the energy axis in the associated graph, the optical band gap energy is computed using the Tauc's plot. An electron and a photon interacting with one another is a crucial aspect of direct transition. On the other hand, a three-particle interaction (photon, electron, and phonon) defines the essential characteristic of an indirect transition to maintain momentum conservation [30]. The band gap spectra and energy values are shown in Figure 2. The band gap energy is 3.46 eV for 1% Ni-doped ZnS nanoparticles and 3.70 eV for 3% nickel doping. Due to the quantum size effect, 3% Ni-doped ZnS has a larger band gap than the bulk ZnS (3.68 eV) [31], [32]. The band gap for 1% Ni-doping is smaller as compared to 3% Ni-doping due to an increase in particle size [33].

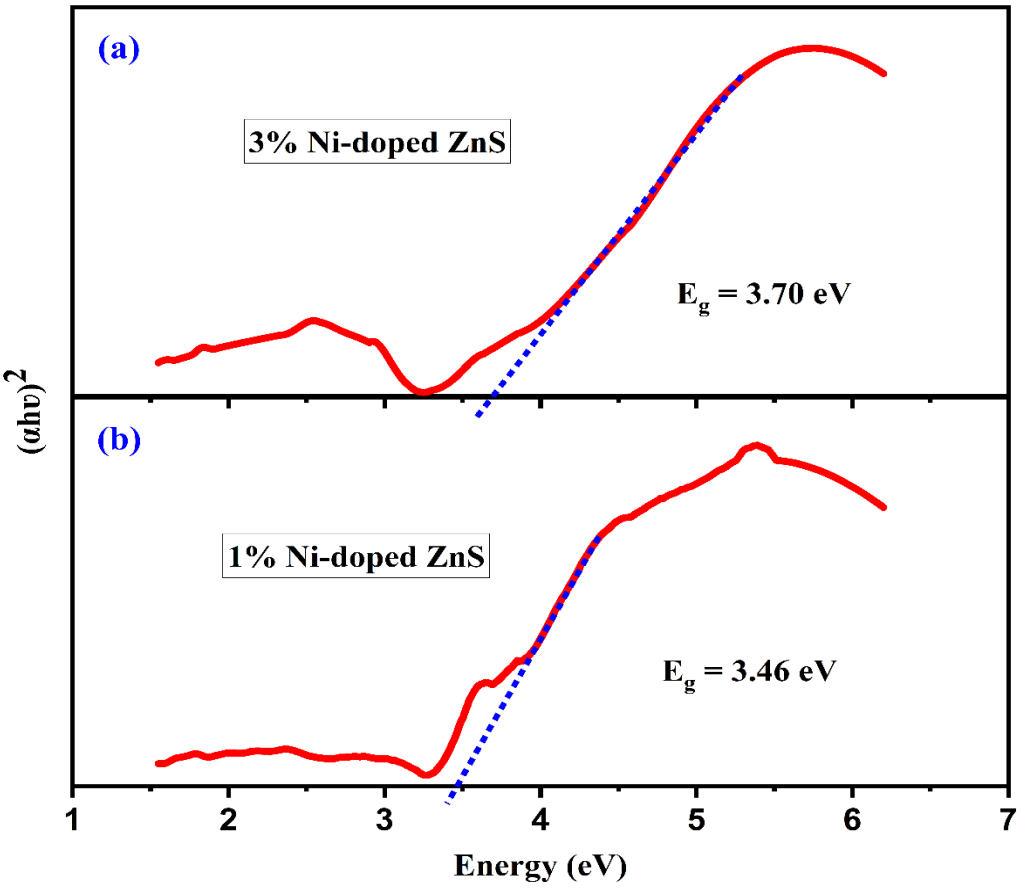

Figure 2. Tauc plot for 1% and 3% Ni-doped ZnS.

3.3 Energy transfer mechanism

Because of their similar ionic radii, Ni2+ ions usually replace Zn2+ ions in the ZnS lattice when Ni is doped into ZnS nanoparticles. This process is called substitutional doping. By producing localized defect sites in the crystal lattice, this substitution modifies the ZnS host's electrical environment and serves as a trap for charge carriers produced during excitation, including electrons and holes. New energy levels related to the 3d orbitals of Ni2+ are introduced into the ZnS band gap by the addition of Ni2+ ions. These states are dependent on the local environment and Ni content and are located below the ZnS conduction band. Electrons in the ZnS valence band absorb energy and move into the conduction band when exposed to light or other excitation sources. Non-radiative relaxation processes and a decrease in total energy may result from certain electrons being trapped in these intermediate energy states in the presence of Ni2+ instead of making it to the conduction band. There are multiple channels involved in the energy transfer mechanism in Ni-doped ZnS. Through dipole-dipole interactions, resonance energy is transferred non-radiatively from the excited ZnS lattice to Ni2+ ions, dimming photoluminescence and decreasing radiative recombination efficiency. Furthermore, local lattice distortions surrounding the Ni2+ sites cause some excess energy to be released as heat through phonon interactions, which affects the nanoparticles' size and crystal structure. When confined in Ni-induced states, electrons may recombine with valence band holes to produce non-radiative relaxation or lower-energy photons. Localized heating effects brought on by these energy transfer and thermalization processes may encourage atomic diffusion and affect the development kinetics of ZnS nanoparticles. First, because of more defect sites and energy dissipation, these activities might promote particle development as the Ni content rises [34], [35]. To sum up, Ni doping in ZnS nanoparticles creates localized energy states that promote energy transfer mechanisms such as nonradiative relaxation and resonance energy transfer. The stability, size, and photophysical characteristics of ZnS nanoparticles are all greatly impacted by these processes [36].

3.4 FTIR analysis of Ni-doped ZnS nanoparticles

At room temperature, nickel-doped zinc sulfide nanoparticles' molecular structure and chemical bonding were investigated by recording their 4000-500 cm-1 spectra. Figure 3 shows the FTIR spectra of Ni-doped ZnS by varying concentrations of Ni doping (1%, 3%). FTIR spectra depict Zinc sulfide nanoparticles' vibrations or Zn-S bonding at around 707 -1022 cm-1 for all the prepared samples. The Zn–OH group and water absorbed in the air are responsible for the wide absorption band with a center at 3560 cm-1 [29]. The vibrational band noted at 1533 cm-1 proves the presence of microstructural formation and C=O stretching vibrations that originate from the molecular adsorption of atmospheric CO2 on the surface of the ZnS: Ni nanosystems [37]. A peak has been observed at 3463 cm-1 due to O-H stretching in all samples because of some absorbed moisture [24]. The infrared absorption frequencies and the tentative vibrational assignments of Ni-doped ZnS nanoparticles are shown in Table 1.

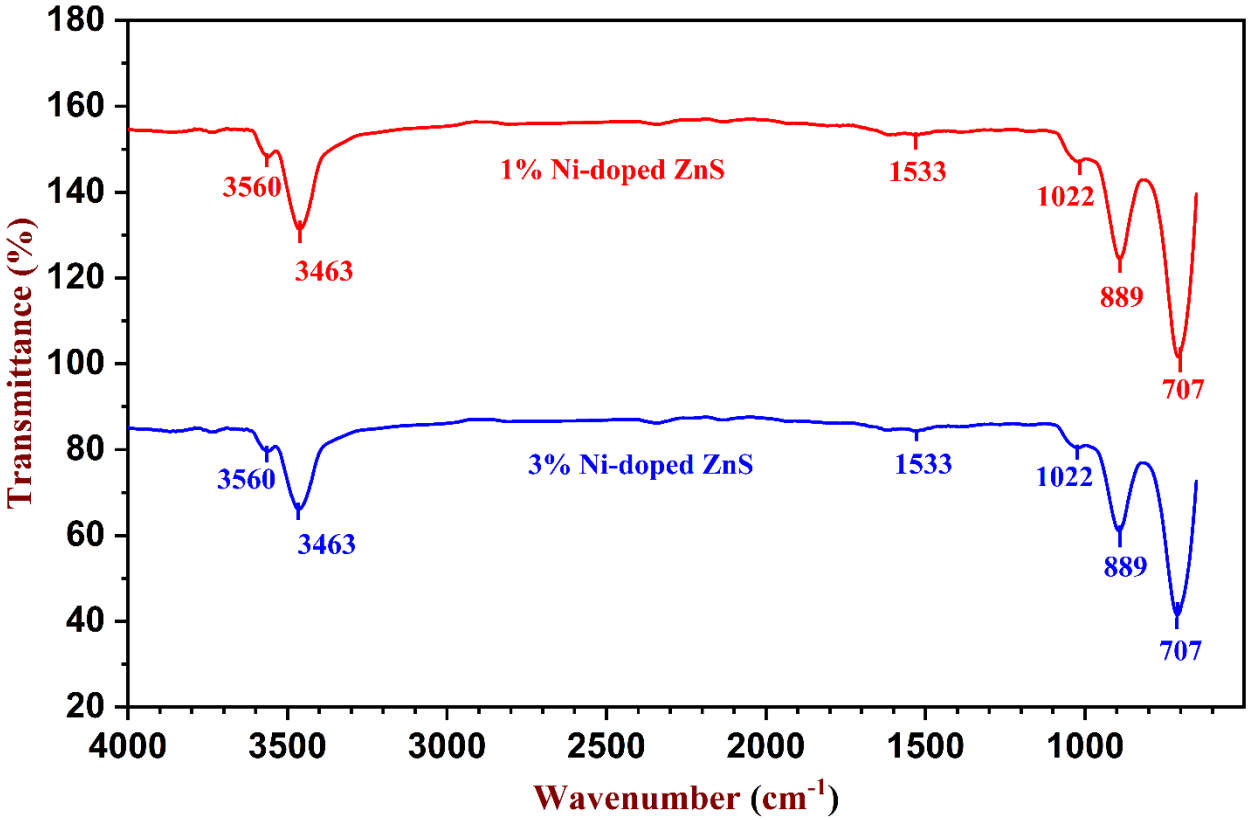

Figure 3. FTIR spectra of 1% and 3% Ni-doped ZnS.

Wavenumber (cm^{-1})	Assignments
3560	Zn–OH group
3463	O-H stretching
1533	C=O stretching
1022	Zn–S bond
707	Cubic ZnS

Conclusion and future perspective

Nickel-doped zinc sulfide nanoparticles were synthesized by using the chemical coprecipitation technique. This technique is effective for producing Ni2+doped ZnS nanoparticles on a wide scale in atmospheric conditions without using expensive equipment. Fourier transform infrared (FTIR) spectroscopy confirmed the presence of characteristic Zn–S bonds and indicated successful Ni incorporation through shifts and variations in the intensity of the vibrational bands. UV-vis spectroscopy demonstrated a blueshift in the band gap with varying concentrations of Ni,

indicating that Ni doping induced changes in the electronic transitions of the ZnS nanoparticles. Additionally, the incorporation of Ni significantly altered the surface area and pore structure of the ZnS nanoparticles, resulting in enhanced photocatalytic performance. These findings highlight the ability of Ni doping to effectively modify the structural and electronic properties of ZnS nanoparticles, making them highly promising for applications in photocatalysis, optoelectronics, and other fields that require specific optical and electronic characteristics. To further optimize these properties for targeted applications, future research should focus on fine-tuning the Ni doping concentration to achieve the desired enhancements.

References

[1] H. Weller, ‘Colloidal Semiconductor Q-Particles: Chemistry in the Transition Region Between Solid State and Molecules’, Angew. Chem. Int. Ed. Engl., vol. 32, no. 1, pp. 41–53, Jan. 1993, doi: 10.1002/anie.199300411.

[2] G. Murali, D. Amaranatha Reddy, R. P. Vijayalakshmi, and R. Venugopal, ‘Structural and Optical Characteristics of Ni Doped ZnS Nanoparticles’, Adv. Mater. Res., vol. 678, pp. 159–162, Mar. 2013, doi: 10.4028/www.scientific.net/AMR.678.159.

[3] M. Hou et al., ‘Synthesis of group II-VI semiconductor nanocrystals via phosphine free method and their application in solution processed photovoltaic devices’, Nanomaterials, vol. 11, no. 8, p. 2071, 2021.

[4] E. A. Slejko and V. Lughi, ‘Size Control at Maximum Yield and Growth Kinetics of Colloidal II–VI Semiconductor Nanocrystals’, J. Phys. Chem. C, vol. 123, no. 2, pp. 1421–1428, Jan. 2019, doi: 10.1021/acs.jpcc.8b07754.

[5] P. E. Lippens and M. Lannoo, ‘Optical properties of II-VI semiconductor nanocrystals’, Semicond. Sci. Technol., vol. 6, no. 9A, p. A157, 1991.

[6] M. P. Sarma and G. Wary, ‘Structural and optical properties of ZnS and Cr-ZnS thin films prepared by chemical bath deposition method’, Am. J. Mater. Sci. Technol., vol. 4, no. 2, pp. 58–71, 2015.

[7] X. Fang et al., ‘ZnS nanostructures: from synthesis to applications’, Prog. Mater. Sci., vol. 56, no. 2, pp. 175–287, 2011.

[8] Y. Zhang, W. Liu, and R. Wang, ‘From ZnS nanoparticles, nanobelts, to nanotetrapods: the ethylenediamine modulated anisotropic growth of ZnS nanostructures’, Nanoscale, vol. 4, no. 7, pp. 2394–2399, 2012.

[9] N. A. Shad et al., ‘Fabrication of Spike-Like Spherical Iron Manganite Nanoparticles for the Augmented Photocatalytic Degradation of Methylene Blue Dye’, J. Electron. Mater., vol. 51, no. 2, pp. 900–909, Feb. 2022, doi: 10.1007/s11664-021-09371-z.

[10] H. Z. Mahmood et al., ‘Plasmon-Based Label-Free Biosensor Using Gold Nanosphere for Dengue Detection’, Crystals, vol. 11, no. 11, p. 1340, Nov. 2021, doi: 10.3390/cryst11111340.

[11] Y. Liu, Y. Li, H. Kang, T. Jin, and L. Jiao, ‘Design, synthesis, and energy-related applications of metal sulfides’, Mater. Horiz., vol. 3, no. 5, pp. 402–421, 2016.

[12] B. Gilbert et al., ‘X-ray absorption spectroscopy of the cubic and hexagonal polytypes of zinc sulfide’, Phys. Rev. B, vol. 66, no. 24, p. 245205, Dec. 2002, doi: 10.1103/PhysRevB.66.245205.

[13] S. P. Patel, J. C. Pivin, A. K. Chawla, R. Chandra, D. Kanjilal, and L. Kumar, 'Room temperature ferromagnetism in Zn1- xCoxS thin films with wurtzite structure', J. Magn. Magn. Mater., vol. 323, no. 22, pp. 2734–2740, 2011.

[14] A. P. Alivisatos, 'Perspectives on the Physical Chemistry of Semiconductor Nanocrystals', J. Phys. Chem., vol. 100, no. 31, pp. 13226–13239, Jan. 1996, doi: 10.1021/jp9535506.

[15] A. Abdel-Kader and F. J. Bryant, 'Blue light emitting ZnS diodes', J. Mater. Sci., vol. 21, no. 9, pp. 3227–3230, Sep. 1986, doi: 10.1007/BF00553360.

[16] Z.-G. Chen, 'Lu, Hui-Ming Cheng', Adv Mater, vol. 22, p. 2376, 2010.

[17] O. K. Echendu and I. M. Dharmadasa, 'Graded-bandgap solar cells using all-electrodeposited ZnS, CdS and CdTe thin-films', Energies, vol. 8, no. 5, pp. 4416–4435, 2015.

[18] Y. Yu et al., 'Ultralow-voltage and high gain photoconductor based on ZnS: Ga nanoribbons for the detection of low-intensity ultraviolet light', J. Mater. Chem. C, vol. 2, no. 18, pp. 3583–3588, 2014.

[19] F. Zhao, I. Kim, and J. Kim, 'Fabrication of the optical fiber pH sensor based on CdSe/ZnS quantum dot', J. Nanosci. Nanotechnol., vol. 14, no. 8, pp. 5650–5653, 2014.

[20] N. A. Shad et al., 'Zn3(VO4)2/Bi2WO6 composite based versatile platform for cotinine sensing and latent fingerprints development by using multiple modalities', Mater. Sci. Eng. B, vol. 301, p. 117203, Mar. 2024, doi: 10.1016/j.mseb.2024.117203.

[21] S. Liu et al., 'Hierarchical ZnS@ C@ MoS2 core-shell nanostructures as efficient hydrogen evolution electrocatalyst for alkaline water electrolysis', Int. J. Hydrog. Energy, vol. 44, no. 47, pp. 25310–25318, 2019.

[22] B. M. Raffah, H. Hassan, M. W. Iqbal, and Y. Al-Hadeethi, 'Synergistic Co-MOF/ZnS Composite: Advancing Supercapattery Performance and Catalyzing Hydrogen Evolution Reaction', Energy Fuels, vol. 38, no. 4, pp. 3477–3490, Feb. 2024, doi: 10.1021/acs.energyfuels.3c04598.

[23] A. A. Othman, M. A. Osman, M. A. Ali, and E. M. M. Ibrahim, 'Influence of transition metals dopant type on the structural, optical, magnetic, and dielectric properties of ZnS nanoparticles prepared by ultrasonication process', Mater. Sci. Eng. B, vol. 270, p. 115195, Aug. 2021, doi: 10.1016/j.mseb.2021.115195.

[24] G. Murugadoss, B. Rajamannan, and V. Ramasamy, 'Synthesis, characterization and optical properties of water-soluble ZnS: Mn2+ nanoparticles', J. Lumin., vol. 130, no. 11, pp. 2032–2039, 2010.

[25] U. Godavarti, V. Mote, and M. P. Dasari, ‘Precipitation derived ZnS:Ni nanocrystals: Study of Structural and Morphological Properties’, Mater. Today Proc., vol. 3, no. 10, pp. 3892–3900, 2016, doi: 10.1016/j.matpr.2016.11.046.

[26] P. Yang et al., ‘Strong green luminescence of Ni 2+ -doped ZnS nanocrystals’, Appl. Phys. Mater. Sci. Process., vol. 74, no. 2, pp. 257–259, Feb. 2002, doi: 10.1007/s003390100889.

[27] P. Baláž, P. Pourghahramani, E. Dutková, E. Turianicová, J. Kováč, and A. Šatka, ‘Mechanochemistry in preparation of nanocrystalline semiconductors’, Phys. Status Solidi C, vol. 5, no. 12, pp. 3756–3758, Dec. 2008, doi: 10.1002/pssc.200780110.

[28] V. D. Mote, Y. Purushotham, and B. N. Dole, ‘Structural, morphological and optical properties of Mn doped ZnS nanocrystals’, Cerâmica, vol. 59, pp. 395–400, 2013.

[29] L. Cao, J. Zhang, S. Ren, and S. Huang, ‘Luminescence enhancement of core-shell ZnS: Mn/ZnS nanoparticles’, Appl. Phys. Lett., vol. 80, no. 23, pp. 4300–4302, 2002.

[30] S. Agrawal, S. K. Sharma, S. Kumar, J. Bahadur, and P. Singh, ‘Size-Dependent Optical and Photo-Catalysis Properties of Microwave Synthesized Zns Nanoparticles Decorated by Site Engineering of Divalent Transition Metals Ions (Mn, Fe, Co & Ni)’, Available SSRN 4726957, Accessed: Sep. 10, 2024. [Online]. Available: https://papers.ssrn.com/sol3/papers.cfm?abstract_id=4726957

[31] R. Raciti, R. Bahariqushchi, C. Summonte, A. Aydinli, A. Terrasi, and S. Mirabella, ‘Optical bandgap of semiconductor nanostructures: Methods for experimental data analysis’, J. Appl. Phys., vol. 121, no. 23, p. 234304, Jun. 2017, doi: 10.1063/1.4986436.

[32] D. A. Reddy, A. Divya, G. Murali, R. P. Vijayalakshmi, and B. K. Reddy, ‘Synthesis and optical properties of Cr doped ZnS nanoparticles capped by 2-mercaptoethanol’, Phys. B Condens. Matter, vol. 406, no. 10, pp. 1944–1949, 2011.

[33] R. Zhang, Y. Liu, and S. Sun, ‘Synthesis and characterization of high-quality colloidal Mn2+-doped ZnS nanoparticles’, Opt. Mater., vol. 34, no. 11, pp. 1788–1794, 2012.

[34] R. Sahraei and S. Darafarin, ‘Preparation of nanocrystalline Ni doped ZnS thin films by ammonia-free chemical bath deposition method and optical properties’, J. Lumin., vol. 149, pp. 170–175, 2014.

[35] A. A. Othman, M. A. Osman, M. A. Ali, W. S. Mohamed, and E. M. M. Ibrahim, ‘Sonochemically synthesized Ni-doped ZnS nanoparticles: structural, optical, and photocatalytic properties’, J. Mater. Sci. Mater. Electron., vol. 31, no. 2, pp. 1752–1767, Jan. 2020, doi: 10.1007/s10854-019-02693-z.

[36] C. Wang, Q. Li, and B. Hu, ‘Preparation and characterization of ZnS nanoparticles prepared by hydrothermal method’, Int. J. Mod. Phys. B, vol. 31, no. 16–19, p. 1744055, Jul. 2017, doi: 10.1142/S0217979217440556.

[37] S. Alhassan, A. H. Alshammari, S. Alotibi, K. Alshammari, W. S. Mohamed, and N. M. A. Hadia, ‘Structural and Optical Properties of Nickel-Doped Zinc Sulfide’, Nanomaterials, vol. 14, no. 19, p. 1599, Oct. 2024, doi: 10.3390/nano14191599.

[38] Priyadharsini N., Elango M., Vairam S., and Thamilselvan M., ‘Effect of nickel substitution on structural, optical, magnetic properties and photocatalytic activity of ZnS nanoparticles’, Mater. Sci. Semicond. Process., vol. 49, pp. 68–75, Jul. 2016, doi: 10.1016/j.mssp.2016.03.033.